Two Water-stable Lanthanide Metal-Organic Frameworks with Oxygen-rich Channels for Fluorescence Sensing Fe(III) ions in Aqueous Solution

Lizhen Liu, [a] Yu, Wang, [a] Rongyan, Lin [a] Zizhu Yao, [a] Quanjie Lin, [a] Lihua Wang, *[,a,] Zhangjing Zhang,*[, a,b] and Shengchang Xiang, [a,b]

[a]*Fujian Provincial Key Laboratory of Polymer Materials, College of Chemistry and Materials Science, Fujian Normal University, 32 Shangsan Road, Fuzhou 350007, PR China*
[b] *State Key Laboratory of Structural Chemistry, Fujian Institute of Research on the Structure of Matter, Chinese Academy of Sciences, Fuzhou, Fujian 350002, People's Republic of China*

Content

1 Materials and measurements

All chemicals were commercially available and used as received without further purification. Elemental analyses of the C, H, and N were carried out on a Vario EL III elementary analyzer. Thermogravimetric analyses (TGA) was performed on a METTLER TGA/ SDTA 851 analyzer under nitrogen atmosphere with heating rate of 10 ^{o}C/min from 30 ^{o}C to 1000 ^{o}C. FT-IR spectra of the synthesized complexes were carried out on a Nicolet 5700 FT-IR spectrometer as KBr pellets. Powder X-ray power diffraction (XRD) patterns were performed on a Rigaku MultiFlex diffractometer at 40 kV, 40 mA for Cu Kα(λ= 1.5406 Å)with a scan speed of 3 deg/min. X-ray photoelectron spectroscopy (XPS) was performed on the Thermo Scientific ESCALab 250Xi using 200 W monochromated Al Kα radiation. The 500 μm X-ray spot was used for XPS analysis. Typically the hydrocarbon C1s line at 284.8 eV from adventitious carbon is used for energy referencing. UV-Vis spectra were recorded on Horiba FluoroMax-4. Inductively coupled plasma (ICP) experiments were performed on Thermo-ICAP6300.

1.1 Synthesis

The ligand H_3L was synthesized according to the literature. [1,2]

Synthesis of {Eu L (H_2O) (DMA)}$_n$ (FJU-13-Eu): A mixture of H_3L (0.02 mmol) and $Eu(NO_3)_2$ (0.04 mmol) was dissolved in 8 mL of DMA/MeOH/H_2O (1:1:0.5) solutions in a glass vial and a small amount of HAc was added to this mixture, and heated at 110 ^{o}C for 48 hours, then cooled to room temperature. Colorless crystals were obtained with 79 % yield based on H_3L, separated by filtration, washed with water and DMA, and then dried in air. Elemental analysis calcd (%) for $C_{27}H_{26}EuNO_{10}$: C 47.94, H 3.87,N 2.07. Found: C 47.36, H 3.91, N 2.17. IR (KBr, cm^{-1}): Fig. 5a): 2915 (mb, γ_{C-H}), 1597 (s, $\gamma_{C=O}$ asymmetric),1421 (s, $\gamma_{C=C}$), 1379 (m, $\gamma_{C=O}$ symmetric), 1178 (s, γ_{C-O}), 1044 (w), 787 (s), 715 (w), 633 (m), 546 (w).

Synthesis of {Tb L (H_2O) (DMA)}$_n$ (FJU-13-Tb): **FJU-13-Tb** was synthesized by a method similar to that of **FJU-13-Eu**, except that $Eu(NO_3)_3$ was replaced by $Tb(NO_3)_3$ and 110 °C was replaced by 80 °C. Colorless crystals were obtained with 49% yield based on H_3L. Elemental analysis calcd (%) for $C_{27}H_{26}TbNO_{10}$: C 47.45, H 3.83,N 2.05. Found: C 45.99, H 3.75, N 2.13. IR (KBr, cm^{-1}): Fig. S2): 2931 (mb, γ_{C-H}), 1578 (s, $\gamma_{C=O}$ asymmetric),1429 (s, $\gamma_{C=C}$), 1382 (m, $\gamma_{C=O}$ symmetric), 1159 (s, γ_{C-O}), 1045 (w), 789 (s), 729 (w), 641 (m), 540 (w).

1.2 Luminescent measurements

The as-prepared sample of **FJU-13-Eu** and **FJU-13-Tb** (~0.2 g) was soaked in ~20 mL of methanol for 1 h, and then the solvent was decanted. Following the procedure of methanol soaking and decanting 10 times, the solvent-exchanged samples were activated by vacuum at 120 °C overnight (~12 h) for the activated **FJU-13a-Eu** and **FJU-13a-Tb,** respectively. To examine the potential of **FJU-13-Eu** and **FJU-13-Tb** for sensing metal ions, the grounded powder sample of the MOF (10 mg) was immersed in 5 mL of different metal ions aqueous solutions, respectively, which were treated by ultrasonication for 0.5 h to form a stable turbid suspension. The corresponding fluorescence emission spectra recorded by a Horiba FluoroMax-4 fluorescence spectrometer. The strongest emission wavelengths for **FJU-13a-Eu** and **FJU-13a-Tb** were located at 616 nm and 545 nm when excited at 320 nm, respectively.

Studies in the simulated physiological conditions. According to the previous literature reports[3-4] HEPES (2-[4-(2-hydroxyethyl)-1-piperazinyl] ethanesulfonic acid) was used as the raw material of the biological solution. The solution (20 mM HEPES aqueous buffer solution (pH = 7)) was prepared by adding 476 mg HEPES into 100 mL water. Then, 10 mg **FJU-13a-Eu** and **FJU-13a-Tb** was introduced into 5.00 mL **Fe^{3+}@HEPES** solutions with different concentrations of Fe^{3+} in the buffered solution and then completing ultrasonic agitation for 30 minutes to form a stable turbid suspension.

1.3 Adsorption measurement

After the bulk of the solvent was decanted, the freshly prepared sample of **FJU-13-Eu** and **FJU-13-Tb** (~0.12 g) was soaked in CH_3OH for 1 hour, and then the solvent was decanted. Following the procedure of CH_3OH soaking and decanting 10 times, the solvent-exchanged samples were activated by vacuum at 120 ^oC until a pressure of 5 μm Hg. 77 K N_2 and 273 K CO_2 adsorption isotherms were measured on Micromeritics ASAP 2020 HD88 surface area analyzer for the guest-free **FJU-13a-Eu** and **FJU-13a-Tb**.

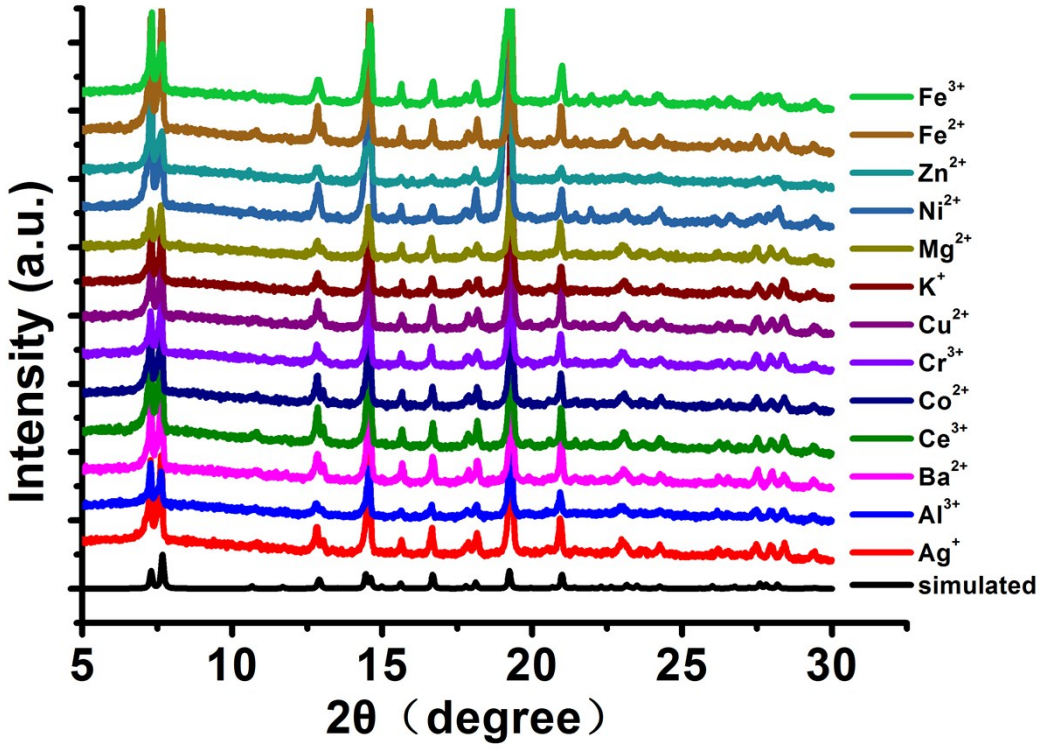

Fig. S1 Powder XRD patterns of **FJU-13a-Eu** after immersing in aqueous solution containing several of metal ions.

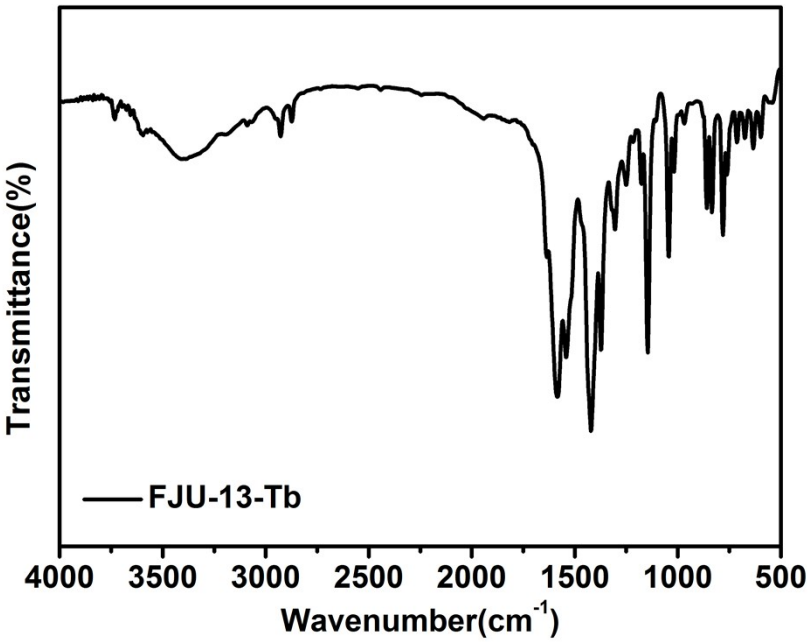

Fig. S2 IR Spectra of **FJU-13-Tb**.

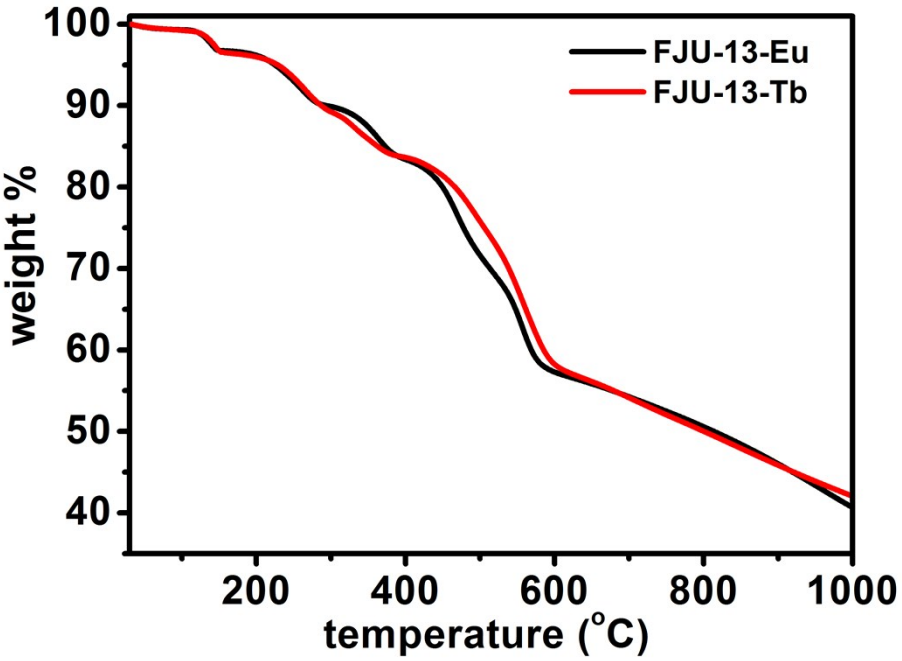

Fig. S3 TG curves for compounds **FJU-13-Eu** and **FJU-13-Tb**.

In order to identify the thermal stability of the two complexes, the thermogravimetric analyses (TGA) have been carried out from 30 to 1000 °C under a N_2 atmosphere. The TGA curves reveal that they possess similar weight loss processes, hence, only the structure of **FJU-13-Eu** is discussed in detail. The TGA curve of **FJU-13-Eu** shows three weight losses. The first weight loss of 3.2 % from 30 to 153 °C was due to lose one coordinated water molecules (calcd 2.7 %). The second weight loss of 6.5 % from 153 to 284 °C was attributed to the loss of the one coordinated DMA molecules (calcd 6.6 %), and the main frameworks begin to slowly decompose.

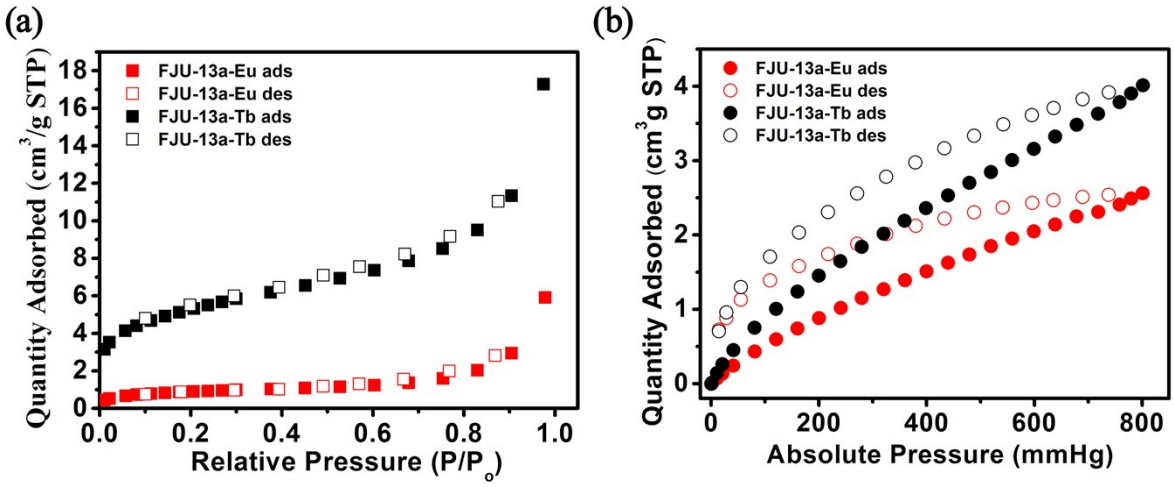

Fig. S4 77 K N_2 adsorption (a) and 273 K CO_2 adsorption (b) in **FJU-13a-Eu** and **FJU-13a-Tb**.

The 77 K N_2 adsorption and 273 K CO_2 isotherms of activated **FJU-13-Eu** and **FJU-13-Tb** were measured, but both of them have low adsorption capability.

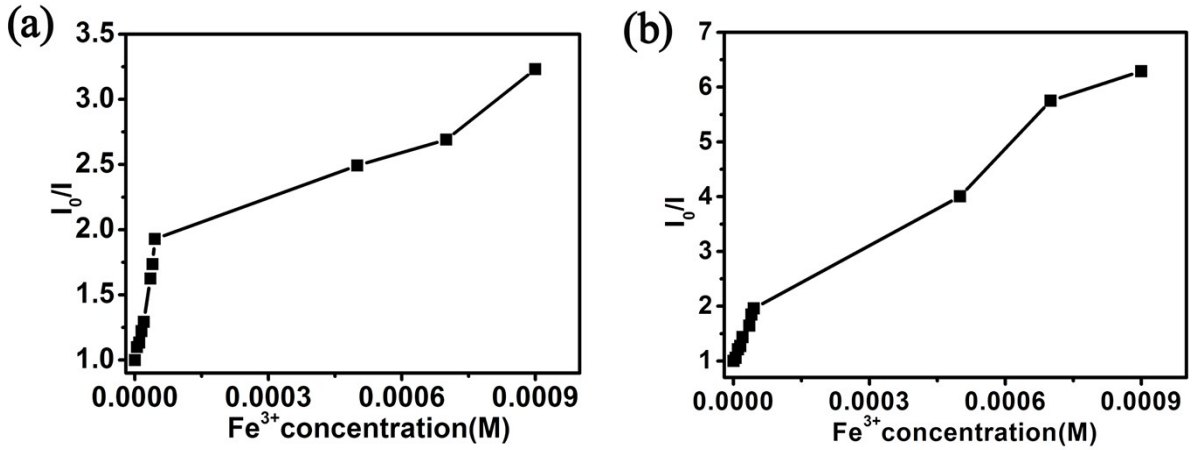

Fig.S5 Concentration-dependent luminescence quenching of **FJU-13a-Eu** (a) and **FJU-13a-Tb** (b) after adding different concentrations of Fe^{3+} ions.

Liquid phase adsorption studies: 30 mg activated **FJU-13-Eu** and **FJU-13-Tb** was added to 15 mL 1mM Fe^{3+} aqueous solution respectively. Samples for analyses were taken from the reaction suspensions and immediately centrifuged to remove the particles. The adsorption of Fe^{3+} was determined using a UV-Vis spectrometer at the maximum absorbance at specified reaction times. The adsorption capacity for Fe^{3+} on MOF is calculated using the following equation: $q_t=[(C_0-C_t)\times V]/m$, where C_0 (mol/L) represent the initial concentration of the Fe^{3+} and C_t (mol/L) represent the concentration of Fe^{3+} at any specified time, V represent solution volume (L), m represent the quality of MOF (g).

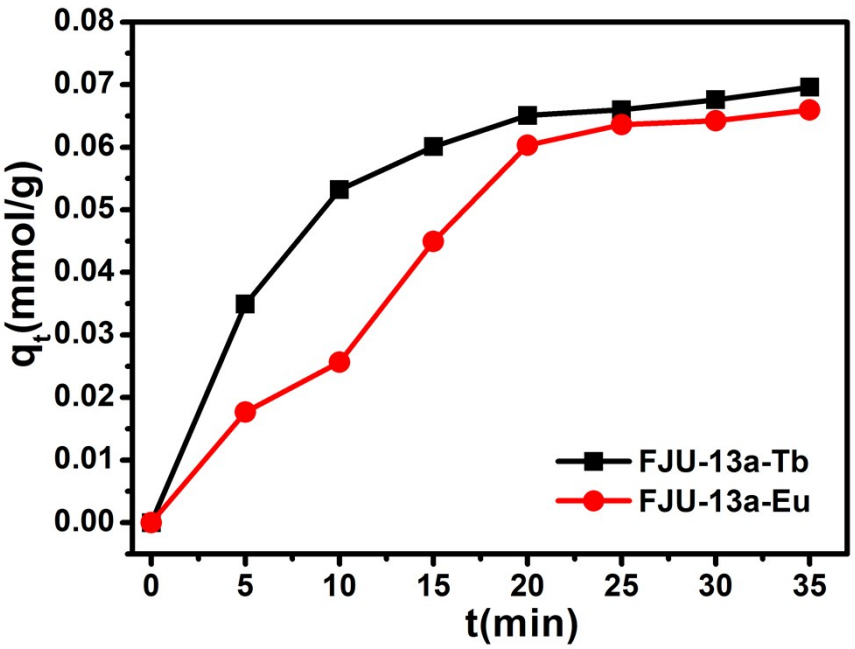

Fig. S6 Time dependent adsorption capacity of 30 mg of **FJU-13a-Eu** and **FJU-13a-Tb** in 15 mL of Fe^{3+} aqueous solution, respectively. The adsorption of iron ions by two MOFs increases with time, and reach adsorption saturation in about 30 min.

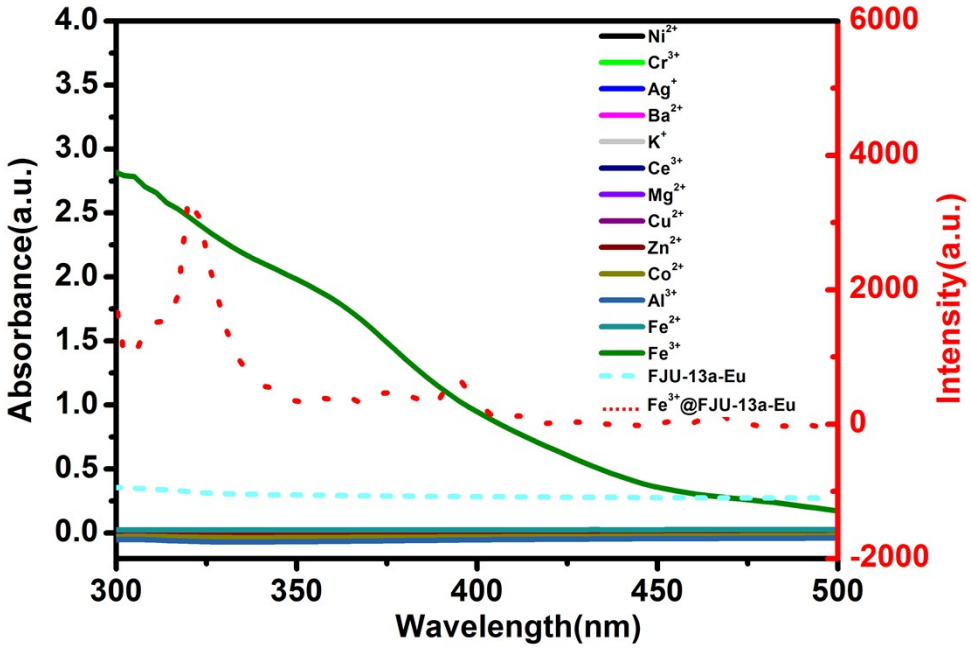

Fig. S7 Solid line: UV-Vis spectra of aqueous solutions containing 1 mM $M(NO_3)_x$ ($M = Ag^{+}$, Al^{3+}, Ba^{2+}, Ce^{3+}, Co^{2+}, Cr^{3+}, Cu^{2+}, K^{+}, Mg^{2+}, Ni^{2+}, Zn^{2+}, Fe^{2+} and Fe^{3+}); Dashed line: UV-Vis spectra of dispersed 10 mg **FJU-13a-Eu** in 5 mL H_2O; Dotted line: Excitation spectra of **FJU-13a-Eu**.

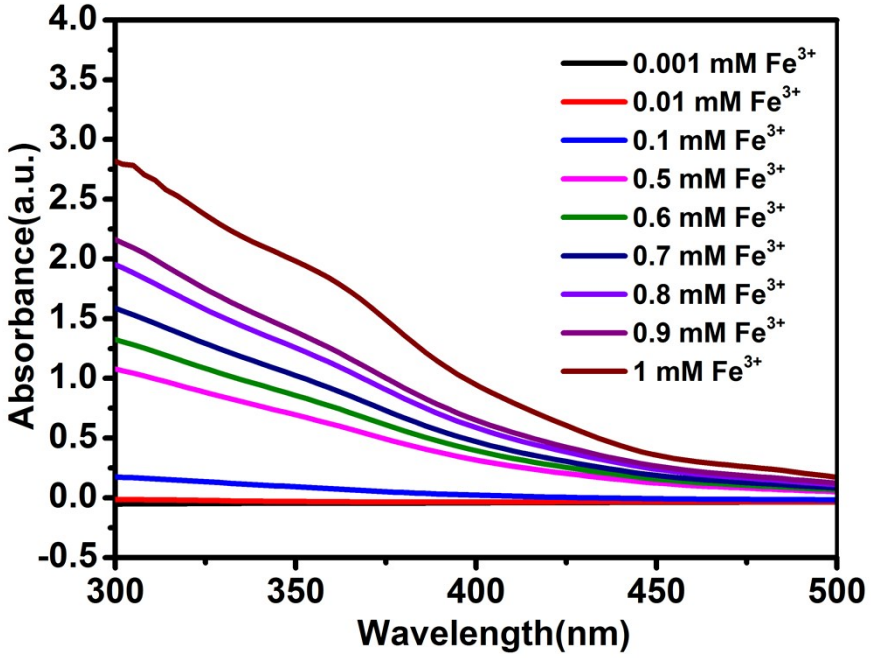

Fig. S8 UV-Vis spectra of aqueous solutions containing different concentration of Fe^{3+}.

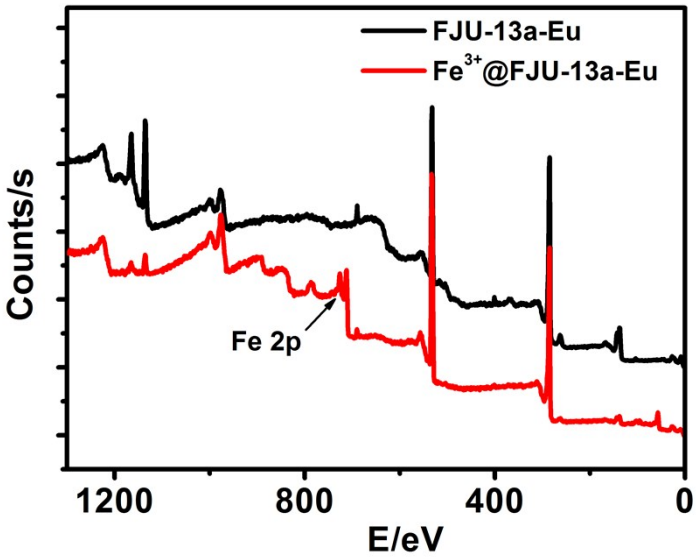

Fig. S9 X-ray photo-electron spectrum of **FJU-13a-Eu** and **Fe^{3+}@FJU-13a-Eu**.

Table S1 Observed Fe^{3+} ion amount in the filtrate solution of MOF **FJU-13a-Eu** before and after the addition of different concentration of $Fe(NO_3)_3$ determined by ICP (Inductively Coupled Plasma).

Concentration of $Fe(NO_3)_3$(M) added to MOF **FJU-13a-Eu**	Observed Eu^{3+} ion amount(mg) in the filtrate solution	Observed Fe^{3+} ion amount(mg) in the filtrate solution	Observed Fe^{3+} ion amount(mg) in solid sample **Fe^{3+}@FJU-13a-Eu** after water washing
0	0.015	0	0
1×10^{-5}	0.0373	0.000288	0.0445
1×10^{-4}	0.013	0.000384	0.083
8×10^{-4}	0.0214	0.0602	0.101
1×10^{-3}	0.0218	0.08416	0.298

(Each 20 mg MOF **FJU-13-Eu** was activated and immersed in 0 M, 1.00×10^{-5} M , 1.00×10^{-4} M, 8.00×10^{-4} and 1.00×10^{-3} M $Fe(NO_3)_3$ aqueous solution, respectively. The filtrate solution was examined by ICP to determine the Fe^{3+} amount. ICP were carried out by Thermo-ICAP6300).

Table S2 Comparison of the detective sensitivity in various Fe^{3+} sensors.

Compound	medium	Stern−Volmer constant K_{sv}(M^{-1})	detection limit	Ref.
FJU-13-Eu	water	2.03×10^4	**1.41 μM**	**This work**
FJU-13-Tb	water	2.11×10^4	**1.01 μM**	**This work**
Eu(4′-(4-carboxyphenyl)- 2,2′:6′,2″-terpyridine)$_3$	water	4.1×10^3	-	5
$[La(TPT)(DMSO)_2]\cdot H_2O$	enthanol	1.36×10^4	-	6
Eu-MOF-LIC-1	DMF	2.87×10^4	-	7
Tb-DSOA	water	3.543×10^3	-	8
$[H(H_2O)_8][DyZn_4(imdc)_4(im)_4]$	DMSO	9.29×10^5	-	9
$[Eu(bpda)_{1.5}]H_2O\}_n$	water	1.25×10^4	0.9 μM	10
$[Eu_2(FDC)_3DMA(H_2O)_3]$ • DMA • $4.5H_2O$	water	1.068×10^4	-	11
$\{[Eu(L)(BPDC)_{1/2}(NO_3)]\cdot H_3O\}_n$	DMF	5.16×10^4	-	12
BUT-14	water	2.17×10^3	3.8 μM	13
BUT-15	water	1.66×10^4	0.8 μM	14
$\{[Eu_2K_2(dcppa)_2(H_2O)_6]\cdot 5H_2O\}_n$	ethanol	4.30×10^4	10^{-6} M	14
$\{[Tb(L)(BPDC)_{1/2}(NO_3)]\cdot H_3O\}_n$	DMF	4.30×10^4	-	13
$[Eu_2(TDC)_3(CH_3OH)_2$• $(CH_3OH)]$	methanol	3.42×10^3	-	15
$[Tb_2(TDC)_3(CH_3OH)_2$• $(CH_3OH)]$	methanol	3.04×10^4	-	16
$[Cd_2 (H_2L)_2(H_2O)_5]$ •$5H_2O$•2DMF	isopropanol	2.23×10^4	-	16
Eu^{3+}@MIL-53-COOH (Al)	water	5.12×10^3	0.5 μM	17
$Eu(atpt)_{1.5}(phen)(H_2O)$	ethanol	7.60×10^3	-	18
Eu_4L_3	DMF	2.94×10^3	10^{-5} M	19
$[Gd_6(L)_3(HL)_2(H_2O)_{10}]\cdot 18H_2O\cdot$x(solvent)	water	7.98×10^2	1.67 ppm	20
$\{[Cd_3(HL)_2(H_2O)_3]\cdot 3H_2O\cdot 2CH_3CN\}_n$	water	1.04×10^4	9.06×10^{-5}M	21
PCN-604	water	8.53×10^3	6.2 μM	22
Tb−MOF	water	16590	10^{-6} M	23

Table S3 Compare the oxygen content of different MOF for detecting iron ions.

Compound	O%[a]	K_{SV} M^{-1}	detection limit	ref
Eu−HODA	28.48	2.09×10^4	6.4 ppb	24
$\{[Eu_2K_2(dcppa)_2(H_2O)_6]\cdot5H_2O\}_n$	20.24	4.30×10^4	10^{-6} M	15
FJU-13-Tb	19.69	2.11×10^4	**1.01 μM**	**This work**
FJU-13-Eu	19.56	2.03×10^4	**1.41 μM**	**This work**
$[Pb_3(BPDP)_{1.5}(OOCC_6H_4COOH)_3]$	17.66	2.23×10^4	-	25
$\{[Cd(5\text{-asba})(bimb)]\}_n$	16.34	1.78×10^4	-	26
[Pb(BPDP)]	15.66	2.2×10^4	-	26
534-MOF-Tb	13.09	5.51×10^3	0.13 mM	27
$\{[Tb_4(OH)_4(DSOA)_2(H_2O)_8]\cdot(H_2O)_8\}_n$	11.67	3.543×10^3	-	28
{[Tb(L)(DMA)]·(DMA)·(0.5H_2O)}	10.89	1.912×10^3	-	29
$[Cd(\mu_6\text{-cpta})_2(py)_2]_n$	5.12	3.096×10^3	0.21 mM	30
$[Gd_6(L)_3(HL)_2(H_2O)_{10}]\cdot18H_2O\cdot$x(solvent)	4.87	7.98×10^2	1.67 ppm	21

[a]oxygen content (%) were calculated from the corresponding exposed oxygen sites in the channels or interlayer of the evacuated framework derived from the crystallographic data.

References

1 L. Z. Liu, Y. X. Ye, Z. Z. Yao, L. Q. Zhang, Z. Y. Li, L. H. Wang, X. L. Ma, Q. H. Chen, Z. J. Zhang and S. C. Xiang, *Chinese Journal of Chemistry*, 2016, **34**, 215.

2 R. Patra, H. M. Titi and I. Goldberg, *New J. Chem,* 2013, **37**, 1494.

3 S. Yoon, E. W. Miller, Q. He, P. H. Do and C. J. Chang, *Angew. Chem., Int. Ed,* 2007, **46**, 6658.

4 Y. Q. Xiao, Y. J. Cui, Q. Zheng, S. C. Xiang, G. D. Qian and B. L. Chen, *Chem. Commun,* 2010, **46**, 5503.

5 M. Zheng, H. Q. Tan, Z. G. Xie, L. G. Zhang, X. B. Jing and Z. C. Sun, *ACS Appl. Mater. Interfaces*, 2013, **5**, 1078.

6 C. Q. Zhang, Y. Yan, Q. H. Pan, L. B. Sun, H. M. He, Y. L. Liu, Z. Q. Liang and J. Y. Li, *Dalton Trans.*, 2015, **44**, 13340.

7 (a) J. S. Costa, P. Gamez, C. A. Black, O. Roubeau, S. J. Teat and J. Reedijk, *Eur. J. Inorg. Chem*, 2008, **10**, 1551; (b) J. N. Hao and B. Yan, *J. Mater. Chem. C*. 2014, **2**, 6758.

8 X. Y. Dong, R. Wang, J. Z. Wang, S. Q. Zang and T. C. W. Mak, *J. Mater. Chem. A*, 2015, **3**, 641.

9Y. F. Li, D. Wang, Z. Liao, Y. Kang, W. H. Ding, X. J. Zheng and L. P. Jin, *J. Mater. Chem. C*, 2016, **4**, 4211.

10 J. Wang, J. R. Wang, Y. Li, M. Jiang, L. W. Zhang and P. Y. Wu, *New J. Chem,* 2016, **40**, 8600.

11 L. Li, Q. Chen, Z. G. Niu, X. H. Zhou, T. Yang and W. Huang, *J. Mater. Chem. C*, 2016, **4**, 1900.

12 W. Yan, C. L. Zhang, S. G. Chen, L. J. Han and H. G. Zheng, *ACS Appl. Mater. Interfaces*,

2017, **9**, 1629.
13 B. Wang, Q. Yang, C. Guo, Y. X. Sun, L. H. Xie and J. R. Li, *ACS Appl. Mater. Interfaces*, 2017, **9**, 10286.
14 H. J. Zhang, R. Q. Fan, W. Chen, J. Z. Fan, Y. W. Dong, Y. Song, X. Du, P. Wang and Y. L. Yang, *Cryst. Growth Des,* 2016, **16**, 5429.
15 K. H. Xu, F. Q. Wang, S. Huang, Z. C. Yu, J. X. Zhang, J. G. Yu, H. Y. Gao, Y. Y. Fu, X. Y. Li and Y. N. Zhao, *RSC Adv,* 2016, **6,** 91741.
16 F. Q. Wang, Z. C. Yu, C. M. Wang, K. H. Xu, J. G. Yu, J. X. Zhang, Y. Y. Fu, X. Y. Li, Y. N. Zhao, *Sensors and Actuators B*, 2017, **239**, 688.
17 Y. Zhou, H. H. Chen, B. Yan, *J. Mater. Chem. A,* 2014*,* **2***,* 13691.
18 Y. Kang, X. J. Zheng, L. P. Jin, *J. Colloid. Interface. Sci*, 2016, **471**, 1.
19 W. Liu, X. Huang, C. Xu, C. Y. Chen, L. Z. Yang, W. Dou, W. M. Chen, H. Yang and S. Liu, *Chem. Eur. J,* 2016, **22**, 18769.
20 Q. H. Tan, Y. Q. Wang, X. Y. Guo, H. T. Liu, Z. L. Liu, *Rsc Adv,* 2016, **6**, 61725.
21W. Q. Tong, W. N. Liu, J. G. Cheng, P. F. Zhang, G. P. Li, L. Hou and Y. Y. Wang, *Dalton Trans*, 2018, **47**, 9466.
22 Y. M. Zhang, X. Y. Yang and H. C. Zhou, *Dalton Trans*, 2018, **47**, 11806.
23 Q. S. Zhang, J. Wang, A. M. Kirillov, W. Dou, C. Xu, C. L. Xu, L. Z. Yang, R. Fang and W. S. Liu, *ACS Appl. Mater. Interfaces*, 2018, **10**, 23976.
24 J. Wang, M. Jiang, L. Yan, R. Peng, M. Huangfu, X. X. Guo, Y. Li and P. Y. Wu, *Inorg. Chem*, 2016, *55*, 12660.
25 B. Xing, H. Y. Li, Y. Y. Zhu, Z. Zhao, Z. G. Sun, D. Yang and J. Li, *RSC Adv,* 2016, **6**, 110255.
26 Y. J. Yang, M. J. Wang and K. L. Zhang, *J. Mater. Chem. C*, 2016, **4**, 11404.
27 M. Chen, W. M. Xu, J. Y. Tian, H. Cui, J. X. Zhang, C. S. Liu, and M. Du, *J. Mater. Chem. C,* 2017, **5**, 2015.
28 X. Y. Dong, R. Wang, J. Z. Wang, S. Q. Zang and T. C. W. Mak, *J. Mater. Chem. A*, 2015, **3**, 641.
29 S. Pal and P. K. Bharadwaj, *Cryst. Growth Des*, 2016, **16** , 5852.
30 J. Z. Gu, X. X. Liang, Y. H. Cui, J. Wu, Z. F. Shi, A. M. Kirillov, *CrystEngComm*, 2017, **19**, 2570.